journal

J. Am. Ceram. Soc., 87 [10] 1843–1847 (2004)

Acicular Mullite Crystals in Vitrified Kaolin

Hong-Yang Lu,*,†,‡ Wei-Lin Wang,† Wei-Hsing Tuan,*,§ and Ming-Hong Lin†,¶

Center for Nanoscience, Institute of Materials Science and Engineering, National Sun Yat-Sen University, Kaohsiung 80424, Taiwan

Department of Materials Science and Engineering, National Taiwan University, Taipei 106, Taiwan

The microstructure of vitrified kaolin ceramic tapes has been studied via scanning and transmission electron microscopy (SEM and TEM). The sintered samples contained crystalline phase of predominantly stoichiometric mullite ($3Al_2O_3{\cdot}2SiO_2$), which consisted of high aspect ratio, acicular crystals that are often referred to as secondary mullite. These crystals were interlocked and embedded in an aluminosilicate glass matrix of inhomogeneous composition. The glass matrix contained an average of ~3.63 wt% K as determined by energy-dispersive X-ray analysis (EDS), whose composition could be approximated to $5Al_2O_3{\cdot}16SiO_2{\cdot}0.1MgO{\cdot}0.3K_2O{\cdot}0.15TiO_2{\cdot}0.12Fe_2O_3$. The acicular crystals have approximately the stoichiometric composition of $Al_2O_3{:}SiO_2 = 3{:}2$. They have grown along a specific crystallographic orientation along the [001] axis. The crystal growth front exhibited facetting on the {110) planes with microfacetting on both the {100) and {010) planes.

I. Introduction

THE crystal structure of mullite is orthorhombic, which belongs to the space group *Pbam* (No. 55). It consists of AlO_6 octahedral chains, parallel to the *c*-axis, which are cross-linked by the $(Al,Si)O_4$ tetrahedral chains. With a large range of solid solution, its chemical composition can vary from $3Al_2O_3{\cdot}2SiO_2$ to $2Al_2O_3{\cdot}SiO_2$ (often referred to as the 3:2 and 2:1 limits,[1] respectively), where the nonstoichiometry is accommodated by oxygen vacancies[2] generated extrinsically.

Triaxial porcelain bodies acquire significant strength and toughness through the formation of mullite during sintering as a result of vitrification. Mullite crystals are categorized by the chemical composition (i.e., nonstoichiometry), and the crystal morphology including both shape and size. Mullite formed from kaolin clay alone is termed primary mullite whereas that formed from reaction with an alkali flux is termed secondary. In vitrified triaxial porcelains[3] of the clay–feldspar–flint composition, mullite crystals of two[4–6] or three[7–9] distinctive morphologies have been reported. Apart from the shape, the crystals can also be differentiated by their size and aspect ratio,[9] and by the chemical composition that changes from the nonstoichiometric 2:1 of primary mullite to the stoichiometric 3:2 of seconday mullite[7] on heating to temperatures higher than 1400°C in triaxial compositions.

Primary mullite (M(I) or type-I, adopting the designations by Iqbal *et al.*[8,9]) of composition close to 2:1,[7] forms only from clay relicts of mostly kaolinite ($Al_2O_3{\cdot}2SiO_2{\cdot}2H_2O$) at 1100°–1150°C[10] as small crystals of <0.5 μm[6] (or <0.1 μm[5,8]) in size. Scaly M(I) crystals[11] forming at lower temperatures are the direct product of clay minerals,[3] and have a characteristic cuboidal shape as observed under the TEM.[7,8] Comer[12] found that primary mullite crystals in a vitrified kaolin, although of the characteristic needle shape, were less than 1 μm long. From the crystal size alone, TEM observations suggested[7] that they were similar to primary M(I)[9] (of scaly appearance) and secondary M(II) (of granular shape). Further, mullite crystals produced in clay–feldspar relicts are secondary mullite (M(II)) with several morphologies, such as the granular, cuboidal,[8,13] acicular, or needlelike.[3,7–9,13] Iqbal *et al.*[7,8] further defined secondary mullite in the fine clay, feldspar, and quartz matrix as type-II and type-III categories based on the aspect ratio.[8,9] They were observed from both model and commercial[9] triaxial porcelains vitrified at temperatures above 1400°C. Tertiary mullite crystals, produced from alumina-rich glass at a later stage of crystallization, had sizes smaller than those of M(I) crystals.[7,9]

The aspect ratio of M(II) crystals depended[9] on the viscosity of the eutectic liquid that varied with the alkali content (e.g., Na_2O versus K_2O) of the initial powder. The cuboidal M(I) crystals appeared to have rounded corners[13] (Fig. 4 in Iqbal *et al.*[7]) as well as facetted surfaces (Fig. 3 in Liu *et al.*[7] and Fig. 5 in Iqabal *et al.*[7]), but the crystallographic facetting was not analyzed.[7,13,14] Whether the cuboidal shape was characteristic of M(I) crystals is ambiguous, since acicular M(II) may appear cuboidal when viewed along the axial direction (i.e., long axis) under the microscope. Further, whether the size and shape of mullite crystals were determined kinetically during precipitation from the melt has not been addressed.

For clarification, we have characterized the mullite crystals in sintered kaolin tapes via XRD, SEM, and TEM. The crystallographic facetting and growth direction of the M(II) crystals were determined. The acicular shape of M(II) in relation to the crystallographic facetting is also discussed.

II. Experimental Procedure

Kaolin powder (Akima-35) was supplied by Associated Kaolin Industries Berhad (Ipoh, Malaysia). The powder containing kaolinite and minor amounts of α-quartz and mica is similar to those used by Castelein *et al.*[10] Its composition, determined via the inductively coupled plasma mass spectrometry (ICP-MS) is SiO_2 (48.6 wt%), Al_2O_3 (35.7 wt%), K_2O (1.2 wt%), Fe_2O_3 (0.9 wt%), TiO_2 (0.4 wt%), MgO (0.2 wt%), CaO (0.1 wt%), and BaO (0.1 wt%).

Green tapes of ~400 μm thick were cast, using a doctor-blade, from a slurry of 20 wt% solid containing 2 wt% Na_3PO_4 (sodium phosphate) dispersant, 2.5 wt% poly(vinyl alcohol) (PVA) binder, and poly(propylene glycol) (PPG) plasticizer in equal quantity. The cast tape has shrunk to a thickness of ~100–150 μm thick after drying. Thin squares of 1.0 cm × 1.0 cm were stamped from the dried tape, placed in a covered alumina setter, and sintered at 1000°C, 1500°, and 1600°C for 1 h at a heating rate of $5°C{\cdot}min^{-1}$.

W. E. Lee—contributing editor

Manuscript No. 186725. Received September 9, 2002; approved June 11, 2004.

This work was funded by the National Science Council of Taiwan through NSC 88-2218-E110-002, 89-2216-E110-036, 90-2216-E110-022, 91-2216-E110-017, 91-2216-E110-018, and 92-2216-E110-003.

*Member, American Ceramic Society.

†National Sun Yat-Sen University.

‡Author to whom correspondence should be addressed. e-mail: hyl@mail.nsysu.edu.tw.

§National Taiwan University.

¶Now with the Department of Mechanical Engineering, National Kaohsiung University of Applied Sciences, Kaohsiung 80728, Taiwan.

Crystalline phases were analyzed using an X-ray diffractometer (XRD, Siemens D-5000, Karshrule, Germany). Sintered samples were mechanically ground and polished with SiC grits successively before diamond lapping to 1 μm of surface roughness for microstructure observations. Grain boundaries were delineated by chemical etching using 1% HF solution. Observations were made via SEM (JEM6400, JEOL™, Tokyo, Japan) when samples were coated with a conducting layer of Au–Pd alloy. Thin foils for TEM were prepared by the standard procedures of mechanically polishing the sintered tape down to ~30 μm thick, dimple-grinding of the center area to <10 μm, and Ar-ion beam thinning to electron transparency. Microstructure analysis for the thin foils was performed using a JEOL™ AEM3010 electron microscope operating at 300 kV.

The chemical compositions of mullite crystals and matrix glass were determined via the energy dispersive spectroscopy unit (EDS, Link Systems, Oxford, England) attached to the TEM and SEM.

III. Results

(1) Crystalline Phases

The crystalline phases in sintered kaolin tapes revealed by XRD are shown in Fig. 1. Mullite (JCPDS 38-0471) started to emerge from sintering at 1000°C for 1 h (trace (a)), and its amount progressively increased with higher sintering temperatures (e.g., trace (b) at 1600°C). The only crystalline phase detected from sintering at 1500° and 1600°C (trace (b)) was mullite.

(2) Microstructures of Secondary Mullite Crystals

(A) General Microstructure via SEM: Crystals of high aspect ratios are characteristic of mullite crystallized from vitrified kaolin, as previously reported.[7–9] General microstructure of samples sintered at 1600°C for 1 h, revealed by secondary electron image (SEI), is shown in Fig. 2(a). The acicular M(II) mullite crystals have grown to ~5–10 μm long and ~0.5–1.5 μm wide. Some of them can be categorized as type II (with an aspect ratio of 3–10) and others as type III (with an aspect ratio of ~30–40), according to Lee and Iqbal.[8,9] The content of high-aspect-ratio mullite crystals was thought to be beneficial to the overall strength and toughness of triaxial porcelain bodies.[9] Having an aspect ratio of ~10–30, these M(II) crystals were much larger and longer than M(I) of ~30 nm[8] found from the clay or clay–feldspar relicts in triaxial porcelains.[7–9] They became randomly interwoven in a glass matrix that had been etched away while preparing the samples for SEM. Some of them have thickened laterally by coalescence (as indicated by unfilled arrow) along the preferred crystallographic growth direction (of [001] as will be shown later). Cuboidal crystals ~0.2–0.5 μm wide, i.e., primary M(I) mullite,[7–9] are also easily found from Fig. 2, as indicated by the arrows. Some of the cuboidal crystals may have been the acicular mullite M(II) observed end-on, as described later.

The coexistence of both types of mullite crystals, the elongated needlelike M(II) and the cuboidal M(I),[7] although the latter was of

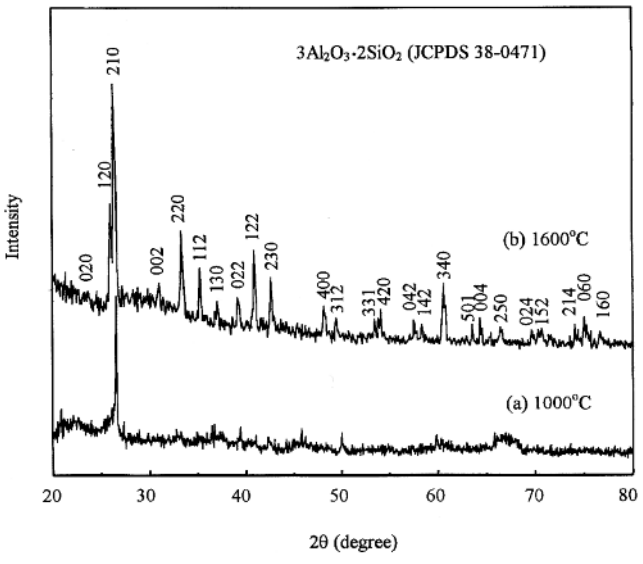

Fig. 1. XRD traces of kaolin samples, sintered at (a) 1000° and (b) 1600°C for 1 h.

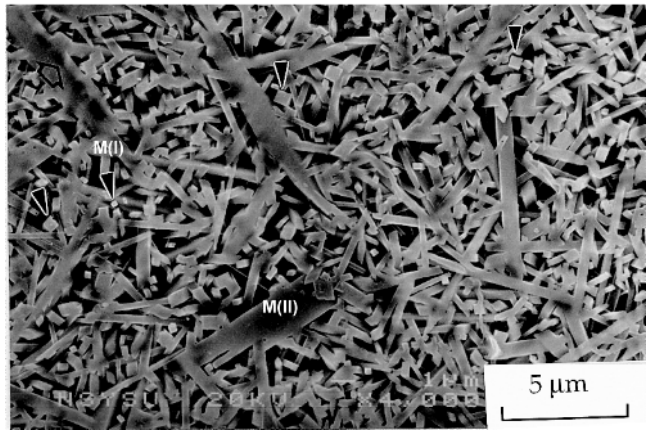

Fig. 2. General microstructure of secondary mullite in samples sintered at 1600°C for 1 h (SEI-SEM).

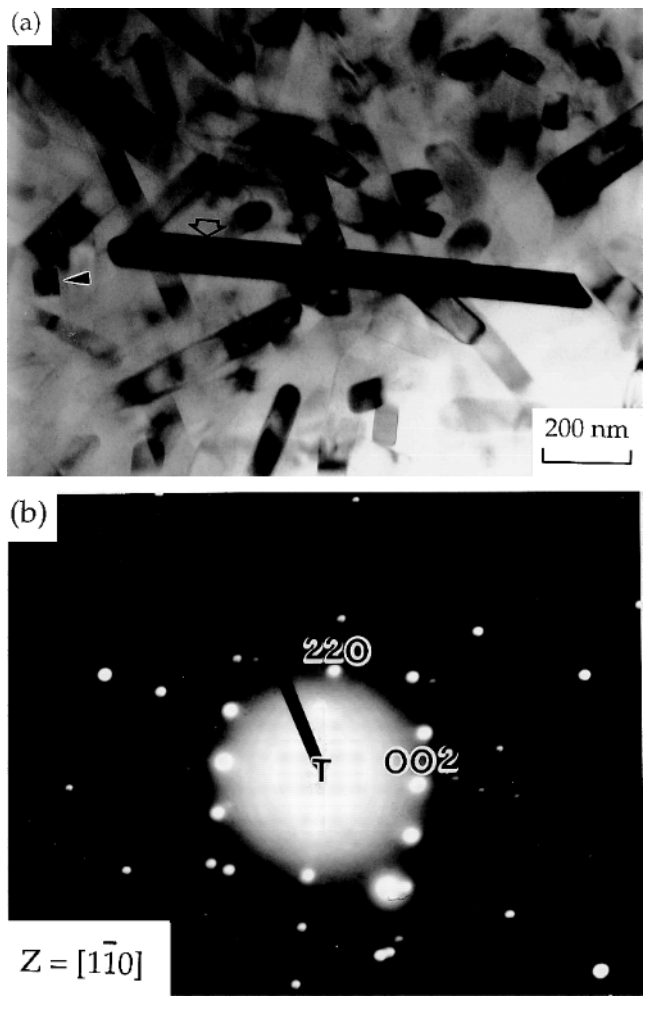

Fig. 3. Acicular mullite crystals randomly oriented and dispersed in a glassy matrix: (a) BF image with (b) the corresponding SADP (TEM).

a minor amount, is confirmed from samples sintered at 1600°C for 1 h.

EDS data taken randomly from six points of the matrix glass gave an average of Al:Si:K:Mg:Ti:Fe = 37.55:55.76:3.63:0.34:0.96:2.06 (wt%) and 39.31:56.34:2.32:0.40:0.57:1.04 (at.%). Correspondingly, the glass composition could be approximated to $5Al_2O_3 \cdot 16SiO_2 \cdot 0.1MgO \cdot 0.3K_2O \cdot 0.15TiO_2 \cdot 0.12Fe_2O_3$. The initial kaolin powder should have contained enough alkali oxides to be self-fluxing at the sintering temperatures. Nevertheless, the concentration of Mg was registered at only one point (0.4 at.%) while others fluctuated considerably. The glass composition was heterogeneous with Al varying between 23.0 and 56.4 at.%, Si between 41.2 and 62.4 at.%, K between 1.11 and 4.66 at.%, Ti between 0.67 and 1.21 at.%, and Fe between 2.91 and 1.50 at.%.

(B) General Microstructure via TEM: The TEM bright-field (BF) imaging reveals that the acicular M(II) crystals, appearing tubular under such imaging conditions, were facetted crystallographically along the two planes (shown by the unfilled arrow in Fig. 3(a)) both parallel to the crystal long axis. The acicular feature has been well represented by the M(II) crystals shown in Fig. 2(a) of SEM-SEI. The M(II) crystals were randomly oriented and dispersed in a glassy matrix that was evidenced by the diffusive halo in the corresponding selected-area electron diffraction pattern (SADP) shown in Fig. 3(b). This is a common observation of samples sintered at 1500° and 1600°C that consisted mostly of M(II) crystals. Crystals of the cuboidal shape, as indicated in Fig. 3(a), are also detected in the field of view. Small, cuboidal crystals of less than ~100 nm × 100 nm (indicated by arrow in Fig. 3(a)) and crystal **B** of ~300 nm × 270 nm (Fig. 4(a)) were all less than 0.5 μm.[7] Both the shape and the size of the crystals were similar to those reported by Liu *et al.*,[14] who thought that only crystals of high aspect ratio and grown in kaolinite (i.e., clay relicts[7,8]) were M(I).

The EDS analysis of six individual acicular crystals has confirmed that the chemical composition of M(II) at an average Al(at.%):Si(at.%) = 72.5:27.5, with slightly SiO_2-rich, can be approximated to the stoichiometric 3:2 mullite. The chemical composition of M(II) was thought to have associated with the eutectic liquid induced by reacting with Na_2O or K_2O feldspar,[9] the feldspar-penetrated clay relicts, from which the mullite crystals were precipitated.[8] Primary mullite M(I) formed initially to the nonstoichiometric composition of Al_2O_3:SiO_2 = 2:1 has grown to secondary mullite on dwelling at sintering temperatures and transformed to the stoichiometric 3:2 mullite M(II).[7–9] The aspect ratio cannot be determined for crystal **B** from such a crystallographic direction. Crystal **A**, however, having an aspect ratio greater than 5, can certainly be categorized to secondary mullite M(II) type II.[7–9]

Some of the acicular crystals, one indicated by the unfilled arrow in Fig. 3(a), appearing dark, were imaged at near the Bragg diffraction condition. Although the M(II) crystals have a long axis lying almost parallel to the image plane, a crystallographic texture[15] exhibiting preferred orientation was not found from SADP (shown in Fig. 3(b)). In fact, some of them (as indicated in Fig. 3(a)) were aligned with the long axis being approximately parallel to the electron beam and, viewing end-on, consequently appeared cuboidal in shape. Such an example is also clearly demonstrated by crystal **B** in Figs. 4(a) and (c).

(C) Crystallographic Facetting: The growth direction of mullite crystals (**A** and **B** in Figs. 4(a–c)) along [001] was determined by tilting the thin foil to Z = [001] and [1$\bar{1}$0],[8] as shown in the corresponding SADPs. Crystals **A** and **B** viewed at the Bragg condition are shown in Figs. 4(b) and (c), respectively, with the corresponding SADP inset. Unlike that reported by Liu *et al.*,[14] these are M(II) crystals judged from both the size and the

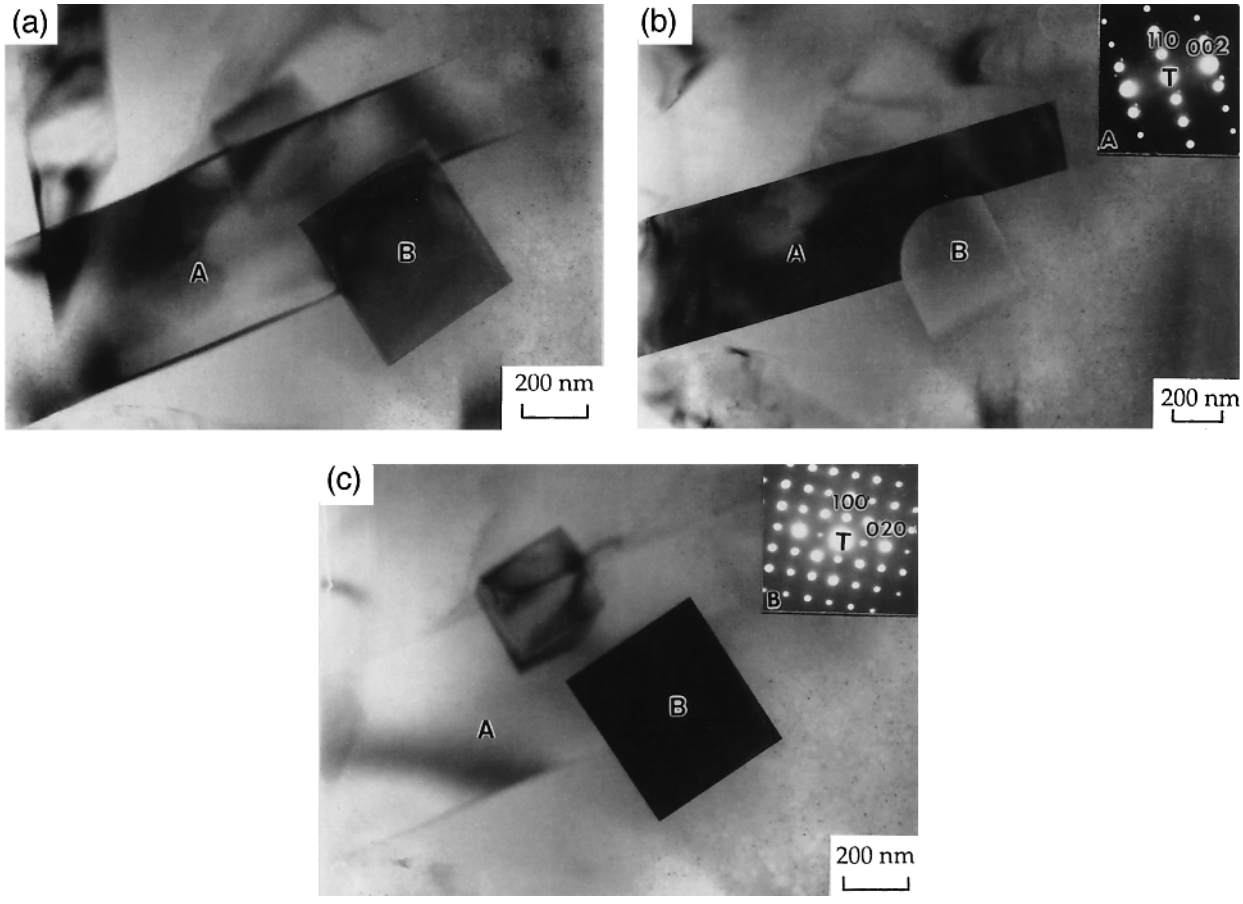

Fig. 4. Acicular mullite crystals from sintering at 1600°C: (a) **A** and **B**, (b) **A**, and (c) **B** at Bragg diffraction condition with the corresponding SADP inset (BF image, TEM).

aspect ratio,[9] although they appear to have distinctive morphologies corresponding to the viewing direction, i.e., the acicular shape of crystal **A** from $Z = [1\bar{1}0]$ and cuboidal shape of crystal **B** from $Z = [001]$.

Crystal **A**, with an aspect ratio greater than ~3–10,[9] viewed from $Z = [1\bar{1}0]$ (shown in Fig. 4(b)), was facetted along (110). The indication is that in contact with a glassy matrix, these facets of the stoichiometric mullite crystals are the crystallographic planes of relatively lower solid-to-liquid surface energy (γ_{sl}). Its long (axial) growth direction along [001] can also be determined.

Crystal **B** exhibiting crystallographic facetting on (110), similar to crystal **A**, is revealed by tilting again to an edge-on imaging condition. As indicated in Fig. 4(c), only the facetted planes are now viewed from $Z = [001]$, i.e., along the axial direction of the crystal. When the crystals are oriented in [001], i.e., the *c*-axis of mullite, they could have easily been mistaken for the cuboidal shape (i.e., crystal **B** in Fig. 4(c)) if the foil had not been tilted to the [110] zone axes under the TEM. Further, because of the small sizes, these crystals could have been mistaken for M(I).

The [001] directions (i.e., *c*-axis) of the two crystals are perpendicular to each other, one of them (crystal **A**) lying on and the other (crystal **B**) perpendicular to the imaging plane. The facetted planes were tilted to an edge-on condition and the crystallographic directions were determined using a technique similar to that for analyzing the residual pores in liquid-phase-sintered Al_2O_3,[16,17] in sapphire,[18] in pressureless-sintered $BaTiO_3$,[19] and the particle form of solid-state-reacted $LiMn_2O_4$ spinel powders.[20]

(D) Crystal Growth Front: The growth of acicular M(II) mullite crystals from eutectic melts along [001] and parallel to the (110) facetted plane (Fig. 4(c)) can be certain. However, the lateral growth edge at the mullite–glass interface did not lie exactly on the (110) plane (as indicated in Fig. 5(a)) on which M(II) crystallized from the melts. It is evidenced from Fig. 5(a) that the facetted planes are in fact corrugated and not atomically flat. The high-resolution image gives the cross-sectional view of a serrated growth front on the (110) plane when viewing from [001], i.e., along the axial direction of an acicular M(II) crystal. It demonstrates that mullite precipitating out from the eutectic liquid has occurred perferentially on the, (110), (100), and (010) planes, as indicated in Fig. 5(a). A view from $Z = [001]$ revealed that these crystals grew laterally, as well as longitudinally on (110) but through steps on the microfacetted planes of (100) and (010) while they were thickened along (110) and lengthened along. [001] Viewing along $[1\bar{1}0]$ (refer to Figs. 5(b) and (c)) revealed that the (110) plane was also corrugated. The lattice fringes of (110) (d_{110} = 0.5390 nm) were clearly resolved, as shown in Fig. 5(b). However, under such imaging conditions, those of (002) (d_{002} = 0.28842 nm) are not delineated and that prevented us from determining the microfacetting, although the surface of the axial growth front again being serrated is evidenced. The SADP corresponding to Fig. 5(b), indicating the axial growth direction along [001], is also shown in Fig. 5(c). The diffuse scattering intensity (SDI, shown by blank arrow), and sideband satellite reflections (detected in both SADPs of Figs. 4(b) and 5(c)) indicating incommensurate modulation,[21] can also be discerned.

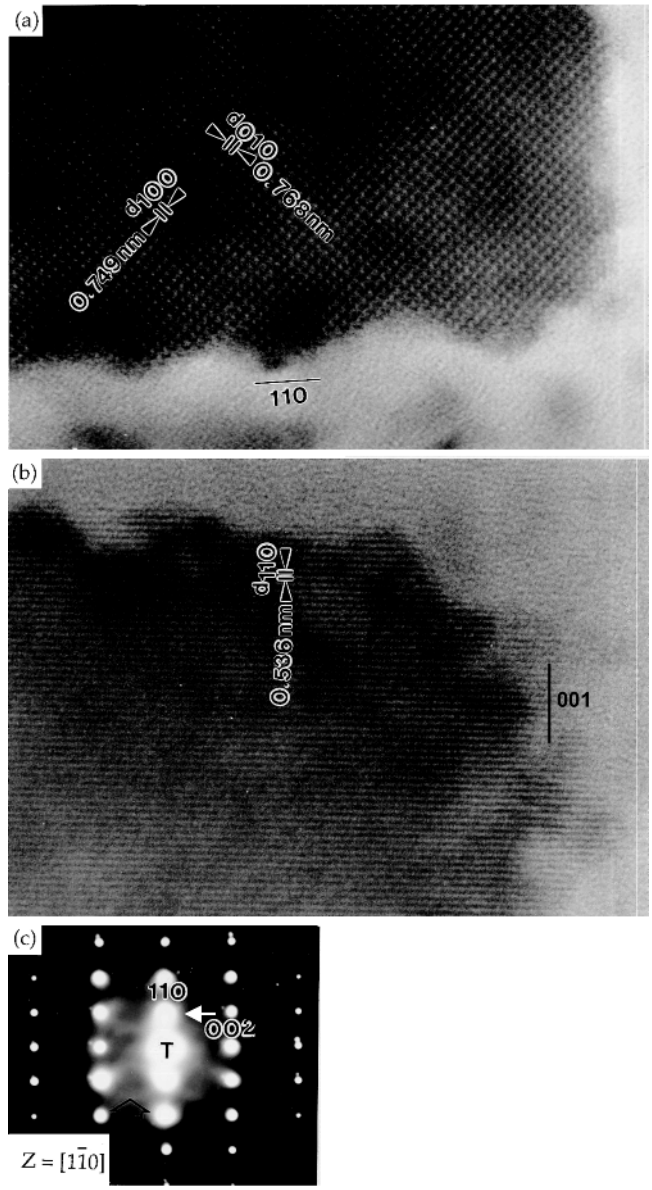

Fig. 5. High-resolution images showing the serrated, lateral growth front of M(II) from (a) the cross-sectional view exhibiting microfacetting on (100) and (010), and (b) the side view exhibiting (110) facet with (c) the corresponding SADP showing diffuse-scattering intensity (TEM).

IV. Discussion

(1) Primary and Secondary Mullite Crystals

Cuboidal mullite crystals (Figs. 2, 3(a), and 4(a)), although smaller in size, are not necessarily M(I).[8] This is because (a) they are aligned along [001] (e.g., crystal **B** in Fig. 4(c)), so their lengths and the aspect ratio cannot be determined and their types are differentiated accordingly, and (b) the firing temperature at 1600°C exceeding 1260°C[1] suggests that they have precipitated out from a transient eutectic liquid similar to those from the clay–feldspar relicts,[7,8,14] rather than a pure kaolinite relict[7,8] that forms M(I).

Both crystals **A** and **B**, although the latter being cuboidal in shape when viewing from $Z = [001]$, are M(II). This is judged by the aspect ratio of crystal **A**, which was greater than 4[9] (as determined from Fig. 4(b)), and the chemical composition of ~3:2 for crystals of similar sizes. The EDS data showing the mullite to be slightly rich in silicon (indicating SiO_2) is due to the overlapping glass.[7]

(2) Formation of Secondary Mullites

In vitrified triaxial porcelains, acicular mullite observed from samples sintered at >1400°C can be M(I) as well as M(II),[9] depending on where, the clay or clay–feldspar relicts,[7–9] these crystals are derived. M(II) is produced by the reaction of clay and feldspar relicts at >1200°C.[3,7] In the absence of feldspar in the starting kaolin powder, M(II) crystals observed in Fig. 2 must have crystallized from liquid melts within the Al_2O_3–SiO_2 system or from those generated by reacting with the alkali impurities, e.g., K_2O,[13] associated with the initial powder and those incurred on processing (i.e., dispersant Na_3PO_4). The M(II) crystals **A** and **B** (Figs. 4(a–c)) obtained from sintering at 1600°C are likely to grow from a eutectic melt formed at >1260°C in the Al_2O_3–SiO_2 system[1] by the reaction of the amorphous silica and alumina that

were derived from the dehydoxylation of kaolinite to metakaolin.[7] The liquid eutectic may also originate from the combination of amorphous Al_2O_3–SiO_2 with the trace impurity of K_2O (~3.63 vs 3.06 wt%[13] detected by EDS) and Na_2O (not detected by EDS). Although sintering of kaolin–Al_2O_3 mixtures, rather than just kaolin, was investigated by Chen *et al.*,[13] precipitation of secondary mullite from glassy phase containing Al_2O_3–SiO_2–K_2O in which a similar amount of 3.06 wt% K_2O detected by EDS was reported. Nevertheless, fine M(I) crystals[7] have not been detected under TEM in the present work and that is probably due to its scarcity.

The growth direction of M(II) crystals along [001] having the low surface energy plane on (110) when precipitating from a eutectic liquid can be certain. Treating the crystal structure as pseudotetragonal with a (0.955 nm) $\approx$ b (0.969 nm), the facetted planes can be addressed as {110}. Microfacetting also occurred on {100} and {010} on M(II) crystallization from the melts resulting in the corrugated growth front along both longitudinal and lateral directions (Fig. 5). The "cuboidal" mullite crystals were distinctively facetted crystallographically, similar to those in Figs. 5 and 7 shown by Iqbal *et al.*[7] The facetting along (110) from their TEM observations, similar to Figs. 4(a–c), could have been determined, but not reported by them. The crystals of the "cuboidal" shape, usually adopted to describe the small and facetted M(I) crystals,[7] are most likely to be M(II), particularly when they are immersed in a glassy matrix.[4–9] The identified acicular nature, the facetting, and the stoichiometry determined by microanalysis all suggest that they are unambiguously M(II) crystals (Figs. 4(a–c)) when viewed from the long morphologic axis, or [001], along which the mullite crystals are grown axially.

Eutectic liquid is necessary for the precipitation of M(II) in vitrified kaolin, i.e., sintered by vitrification. The amount of liquid formed at sintering temperatures, and the duration at which the crystallization has taken place, will determine the chemical composition and the aspect ratio of M(II). Consequently, the aspect ratio (that differentiates type II from type III[9]) was controlled kinetically as they were grown from the melts. Indeed, reports have suggested that the shape and size are affected by both heating rate[22] and annealing temperature.[23] If a liquid eutectic is made available, M(II) would then retain the acicular shape and grow in size irrespective of the sintering temperature. Although the aspect ratio is a strong function of viscosity,[7] the characteristic acicular morphology of M(II) has been developed due to the anisotropic solid-to-liquid surface energy between the mullite crystal and ther eutectic liquid. The M(II) crystals exhibit crystallographic facetting when the total surface energy is minimized toward the thermodynamic equilibrium.

V. Conclusions

Ceramic tapes prepared from a commercial kaolin powder, sintered at 1500° and 1600°C, have been characterized by the microstructure of interlocking acicular, secondary mullite (M(II)) crystals embedded in a glassy matrix. The M(II) crystals growing axially along [001] from liquid eutectic melts of compositions lying in the Al_2O_3–SiO_2 and K_2O(–Na_2O)–Al_2O_3–SiO_2 systems. They have exhibited crystallographic facetting on the corrugated {110} planes with microfacetting on {100) and {010) planes. This suggests that {110) are the planes of low solid-to-liquid surface energy in the stoichiometric M(II) crystals.

References

[1]I. A. Aksay and J. A. Pask, "Stable and Metastable Equilibria in the System SiO_2–Al_2O_3," *J. Am. Ceram. Soc.*, **58** [11–12] 507–12 (1975).

[2]T. Epicier, "Benefits of High-Resolution Electron Microscopy for the Structural Characterization of Mullites," *J. Am. Ceram. Soc.*, **74** [10] 2359–66 (1991).

[3]W. M. Carty and U. Senapati, "Porcelain—Raw Materials, Processing, Phase Evolution and Mechanical Behavior," *J. Am. Ceram. Soc.*, **81** [1] 3–20 (1998).

[4]S. T. Lundin, "Electron Microscopy of Whiteware Bodies," *Trans. Int. Ceram. Congr.*, **4**, 383–90 (1954).

[5]K. H. Schuller, "Reactions between Mullite and Glassy Phase in Porcelains," *Trans. Br. Ceram. Soc.*, **63** [2] 102–17 (1964).

[6]S. T. Lundin, "Microstructure of Porcelain," *Natl. Bur. Stand. (U.S.) Misc. Publ.*, **257**, 93–106 (1964).

[7]Y. Iqbal and W. E. Lee, "Fired Porcelain Microstructures Revisited," *J. Am. Ceram. Soc.*, **82** [12] 3384–90 (1999).

[8]Y. Iqbal, and W. E. Lee, "Microstructural Evolution in Triaxial Porcelain," *J. Am. Ceram. Soc.*, **83** [12] 3121–27 (2000).

[9]W. E. Lee, and Y. Iqbal, "Influence of Mixing on Mullite Formation in Porcelain," *J. Eur. Ceram. Soc.*, **21** [14] 2583–86 (2001).

[10]O. Castelein, R. Guinebretiere, J. P. Bonnet, and P. Blanchart, "Shape, Size and Composition of Mullite Nanocrystals from Rapidly Sintered Kaolin," *J. Eur. Ceram. Soc.*, **21** [14] 2369–76 (2001).

[11]K. H. Schuller and H. Kromer, "Primary Mullite as a Pseudomorph after Kaolinite"; pp. 533–38 in Proceedings of the International Clay Conference (Mexico City, 1975). Edited by S. W. Bailey. Applied Publishing, Wilmette, IL, 1976.

[12]J. J. Comer, "Electron Microscopy of Mullite Development in Fired Kaolinite," *J. Am. Ceram. Soc.*, **43** [7] 378–84 (1960).

[13]Y. F. Chen, M. C. Wang, and M. H. Hon, "Secondary Mullite Formation in Kaolin–Al_2O_3 Ceramics," *J. Mater. Res.*, **19** [3] 806–14 (2004).

[14]K. C. Liu, G. Thomas, A. Caballero, J. M. Moya, and S. DeAza, "Mullite Formation in Kaolinite–α-Alumina," *Acta Metall. Mater.*, **42** [2] 489–95 (1994).

[15]C. Y. Chen and W. H. Tuan, "Evolution of Mullite Texture on Firing Tape-Cast Kaolin Bodies," *J. Am. Ceram. Soc.*, **85** [5] 1121–26 (2002).

[16]C. A. Powell-Dogan and A. H. Heuer, "Microstructure of 96% Alumina Ceramics: I, Characterization of the As-Sintered Materials," *J. Am. Ceram. Soc.*, **73** [12] 3670–76 (1990).

[17]M. P. Mallamaci and C. B. Carter, "Facetting of the Interface between Al_2O_3 and Anorthite Glass," *Acta Mater.*, **46** [8] 2895–907 (1998).

[18]J. H. Choi, D. Y. Kim, B. J. Hockey, S. M. Wiederhorn, C. A. Handwerker, J. E. Blendell. W. C. Carter, and A. R. Rossen, "Equilibrium Shape of Internal Cavities in Sapphire," *J. Am. Ceram. Soc.*, **80** [11] 62–68 (1997).

[19]J. K. Liou, M. H. Lin, and H. Y. Lu, "Crystallographic Facetting in Sintered $BaTiO_3$," *J. Am. Ceram. Soc.*, **85** [12] 2931–37 (2002).

[20]M. R. Huang, C. W. Lin, and H. Y. Lu, "Crystallographic Facetting in Solid-State-Reacted $LiMn_2O_4$ Powder," *Appl. Surf. Sci.*, **177**, 103–13 (2001).

[21]B. D. Butler, T. R. Welberry, and R. L. Withers, "Oxygen Vacancy Ordering and the Incommensurate Structure of Mullite," *Phys. Chem. Miner.*, **20**, 323–32 (1993).

[22]O. Castelein, B. Soulestin, J. P. Bonnet, and P. Blanchart, "The Influence of Heating Rate of the Thermal Behaviour and Mullite Formation from a Kaolin Raw Material," *J. Eur. Ceram. Soc.*, **27** [5] 517–22 (2001).

[23]B. R. Johnson, W. M. Kriven, and J. Schneider, "Crystal Structure Development during Devitrification of Quenched Mullite," *J. Eur. Ceram. Soc.*, **21** [14] 2541–62 (2001). □